

## **SYNTHESIS, CHARACTERIZATION AND PHOTOCATALYTIC ACTIVITY OF TiO<sub>2</sub> NANOTUBE PRODUCED AT VARIOUS VOLTAGE**

Srimala Sreekantan, Roshasnorlyza Hazan and Zainovia Lockman

*School of Materials & Mineral Resources Engineering,  
Universiti Sains Malaysia, Engineering Campus, 14300 Nibong Tebal,  
Seberang Perai Selatan, Pulau Pinang, Malaysia*

### **ABSTRACT**

The formation of self-organized TiO<sub>2</sub> nanotubes was investigated by anodizing titanium foils in electrochemical bath containing 1 M glycerol with 0.7 g NH<sub>4</sub>F. The bath consisted of 2 electrodes; titanium foil as a working electrode and platinum plate as a counter electrode. The pH of the bath was kept constant at pH 6 and potential applied on the electrode was varied from 5 V to 30 V in an interval 5V. This is done to investigate the effect of voltage on the nanotubes formation. It was found that the self-organized TiO nanotubes with different diameter size (20-80 nm) can be successfully established by simple altering the anodization voltage. For as-anodized sample, the self-organized TiO<sub>2</sub> nanotubes have amorphous structure and annealing at 400°C of the nanotubes promotes formation of anatase and rutile phase. Photocatalytic activity of the self-organized TiO<sub>2</sub> nanotube with various sizes was evaluated by measuring the degradation of methylene orange. The elaboration of this observation is described in detail in this paper.

### **INTRODUCTION**

Recent, water and air pollution [1] has attracted a great deal of researcher attraction in finding solution for environmental purification. Variety method of environmental purification [1-4] such as biological treatment and physical method (chlorination and adsorption) was used. The biological treatment only adsorbed dyes on the sludge and are not degraded. Also, physical methods just simply transfer the pollutants to another phase rather than destroying them [5]. Among them, environmental purification using photo catalyst offers great advantages as compared to other methods [1,2]. Photocatalyst means a function that substances work as catalyst if light exists. If light reaches photocatalyst materials, electron is excited from the valance band to conduction band, leaving the hole in valance band [6]. These holes produce hydroxy radicals (+OH) to oxidation of H<sub>2</sub>O and electrons are transferred to oxygen to produce superoxide anions (O<sup>2-</sup>) during the photo-illumination at the semiconductor surface. These oxidants (or reductants) decompose organic pollutant into CO<sub>2</sub> and H<sub>2</sub>O [5]. The efficiency of photocatalytic very much related to structure and physical properties of semiconductors materials surfaces [3]. Recently, nanotube structures were found to be having high surface area, high oriented and long-nanotubes [7]. Large contact surface exposed to pollutant molecules offers the reaction rate of photocatalytic reactions [8] because it is promotes greater amount of catalytic sites [9] than a dense surface [10]. In conjunction

with this, Awitor et al. [2] has observed that strong photocatalytic activity can be achieved by exposing the pollutant to TiO<sub>2</sub> nanotubes layers. Therefore, in this work the formation of TiO<sub>2</sub> nanotube via anodization were explored. To date, there are few article reports on the formation of TiO<sub>2</sub> nanotubes in fluoride contain electrolyte [11,12]. It is evident that the dimensions of the tube-layers, such as diameter and thickness, strongly depend on the electrochemical conditions used [11]. An extensive effort was done to study TiO<sub>2</sub> as photocatalyst operating under irradiation of UV light [13]. TiO<sub>2</sub> nanotubes also demonstrated promising in methyl orange degradation [5].

Therefore, in this paper, a detailed study have been performed to evaluate the diameter of the nanotubes produced from 5 V to 30 V and appropriate microstructure characteristic and morphology, allowing its application as photocatalyst in degradation of methyl orange aqueous solution.

## **EXPERIMENTAL**

High purity titanium foils (99.6% purity) of thickness 0.1 mm that was used in this study were purchased from STREM Chemicals. Anodization was done in a standard two-electrode bath with titanium as the working electrode and platinum as the counter electrode. Prior to anodization, Ti foils were degreased by sonicating in acetone for 15 minutes followed by rinsing in deionised water and then dried in nitrogen stream. After drying, the foil was exposed in the electrolyte which consists of 1 M glycerol with 0.7 g NH<sub>4</sub>F. The pH of the bath was kept constant at pH 6. The anodic potential was varied from 5 V to 30 V with sweep rate at 1V/min. The bath was kept at room temperature. After the anodization was completed, the titanium foil was annealed at 400 °C in an air atmosphere furnace for 2 hours. It is anticipated that the formation of crystalline phase will lead to enhanced photodegradation activity.

The morphologies of the anodized titanium were characterized using a Field Emission Scanning Electron Microscope (FESEM SUPRA 35VP ZEISS) operating at working distances down to 1 mm.

The photocatalytic degradation studies was performed by dipping 5 pieces of 3 cm<sup>2</sup> titanium foil which was dipped in 200 ml of 50 ppm methyle orange in self-constructed photoreactor which consist of a quartz glass. The details regarding the photocatalytic degradation have been reported elsewhere [14].

## **RESULT AND DISCUSSION**

In the present work, the anodization potential voltages were ramp up from 0 V to a desired potential and holding for 1 hour. The current densities for different anodization voltage were shown in Figure 1. From the graph, it was noticed that the current density were increase with increasing the applied potential from 5 V to 30 V because the amplitude of oscillations was increased [15]. The current drops rapidly in the first stage, typical for a classical high-field passivation behavior that leads to the formation of

compact oxide film [16] and this attributed to active component selective dissolution on the top surface layers before the surface is depleted [17]. After the initial stage, current increase to a certain maximum value, which can be ascribed to a random drilling of pits and converted to a porous worm-like initial layer (the latter is combined with an increase in the active surface area) due to localized dissolution of the oxide [18]. As evident from Figure 1, after the potential reaches target value, anodic current decreases gradually until it reaches a steady state and maintain with anodizing time [19]. At this final stage, the structure become self-orientated, reduce active area and stable shape of pores was established (result in dissolution and oxidation rate). It could be explained on the basis of the different anodic conditions employed lead to a less passivation of the Ti substrate, so that the less aggressive nature of the organic non-acidic electrolyte [16].

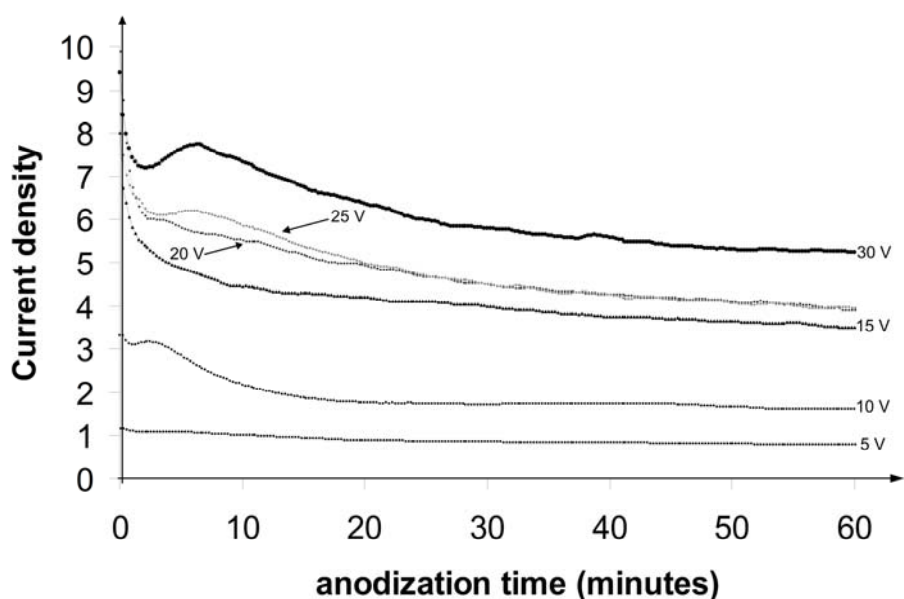


Figure 1: Current density curve for anodization of Ti foils in 1 M glycerol + 0.7 g at (a) 5V (b) 10 V (c) 15 V (d) 20 V (e) 25 V and (f) 30 V for 1 hour.

Figure 2 shows the XRD patterns of sample consisting of as-prepared arrays of tubes (Figure 2 a) and after annealing in air at 400 °C for 2 h (Figure 2 b). The result indicates as-anodized self-organized TiO<sub>2</sub> nanotubes have amorphous structures, which can be transformed to anatase upon annealing. XRD measurements revealed that the annealed nanotubes have anatase structure; some Ti-peaks from the Ti substrate are observed. The predominant anatase phase is (101), (200) and (211) phases are detected.

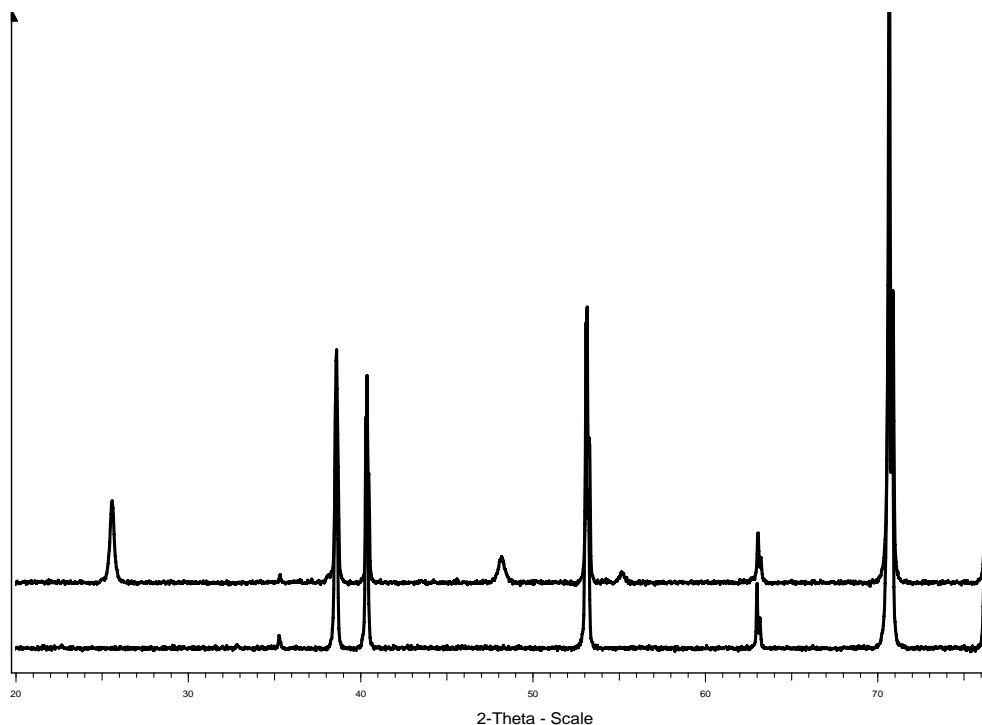


Figure 2: XRD pattern of the TiO<sub>2</sub> nanotubes (a) as-prepared; (b) annealed for 2 hours at 400°C [Ti: titanium, A: anatase]

Generation of self-assembled TiO<sub>2</sub> nanotubes in a highly regular arrangement was achieved by anodizing Ti foils in fluoride electrolyte at different voltages ranging from 5 to 30 V, thus precisely controlling tube diameter. Figure 3 shows SEM micrograph of self-assembled TiO<sub>2</sub> nanotube layers of different inner diameters from 16 nm to 82 nm, that were grown on titanium foils by anodization in the fluoride electrolyte at potentials from 5 V to 30 V. It is well known that the diameters of the nanotube made by anodization method increased when the anodization voltages were increased and the trend start to remain almost constant after 25 V (Figure 4). The SEM images of TiO<sub>2</sub> nanotubes showed that Ti foil anodized at a low voltage of 5 V for 1 hour had only pit (insert in Figure 3(a)). Complete tubes structures with well-alligned nanotubes array were produced at 10 V due to sufficient electrical potential to well develop the TiO<sub>2</sub> nanotubes arrays on the Ti surface. At a low anodic potential range (Figure 3a), the arrangement of the self-organized nanotube was irregular, whereas a higher applied potential facilitated the formation process of anodic TiO<sub>2</sub> nanotubes up to 10 V after which the arrays of the self-organized nanotubes became stable and gradually changed to a regular pattern. Meanwhile, at the higher applied potential of more than 20 V at which the nanotubes array reached an optimum, the morphologies of the self-organized nanotubular layer became irregular again. These results indicated that the formation of the well-alligned TiO<sub>2</sub> nanotube arrays at the voltage of below 10 V was difficult due to weak electrochemical etching reaction and the best array of TiO<sub>2</sub> nanotubes was obtained under an applied potential of 10 V to 20 V in glycerol electrolyte as represented in Figure 3 (b-d).

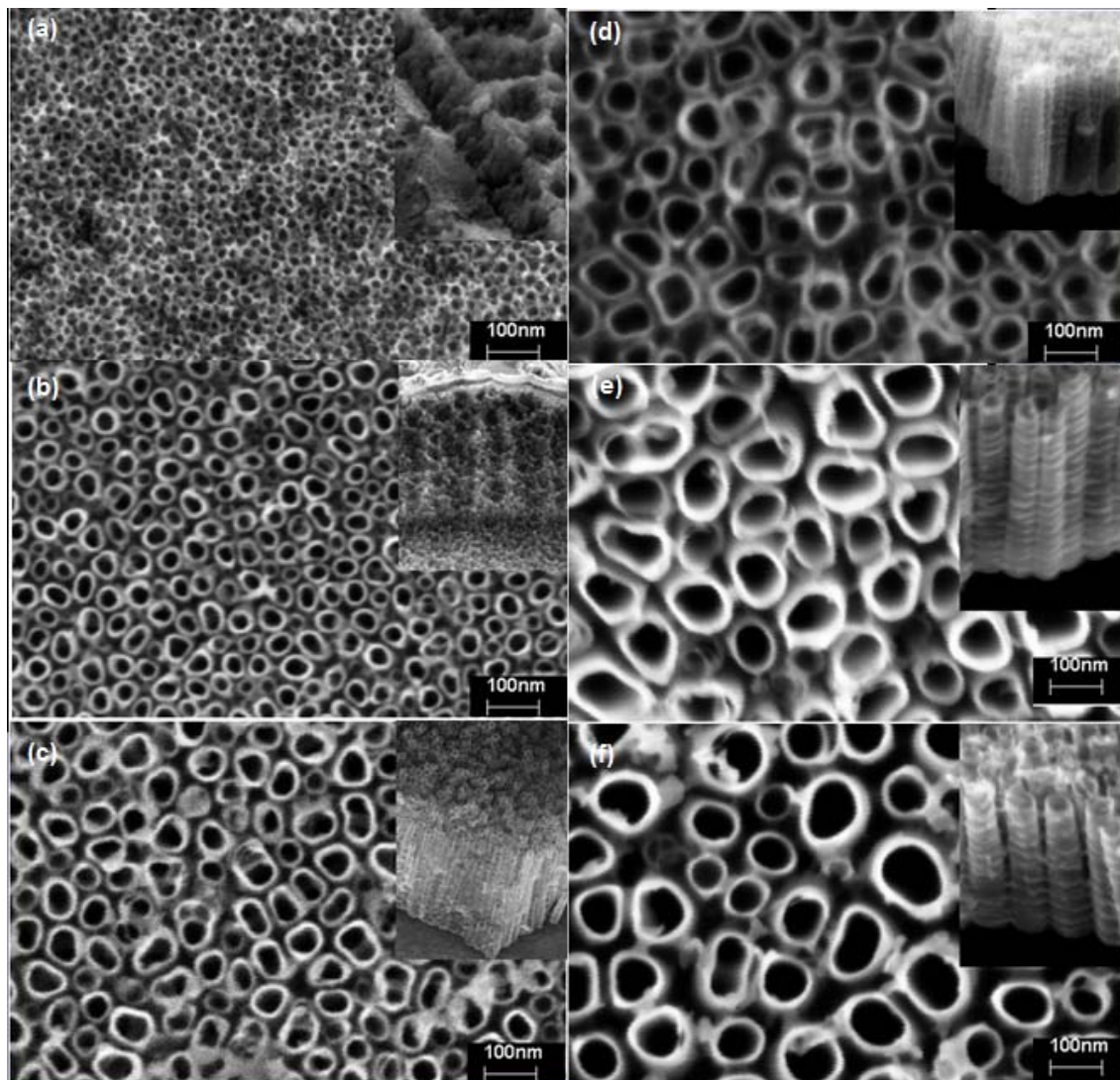


Figure 3: FESEM image of Ti foil anodized for 1 hour at different applied voltage (a) 5 V, (b) 10 V, (c) 15 V, (d) 20 V, (e) 25 V and (f) 30 V

Figure 5 shows the percent of methyl orange degraded by existence of  $\text{TiO}_2$  nanotubes. Nanotubes produced at 15 V show the greatest degradation over the rest of another sample produced at different voltages followed by 20, 25 and 30 V. This is due to high surface area [1] given by these nanotubes allow more aqueous reactants to be adsorbed onto the outer and also inner surfaces [12]. However, nanotubes that produced at 5 V and 10 V with inner diameter of 16 nm and 28 nm respectively show opposite result. This is because the mouths of the nanotubes were too small for methyl orange molecules to get into and promote the degradation. Also from this result, the critical inner diameter for the methyl molecules to penetrate the nanotubes is between 28 nm and 46 nm.

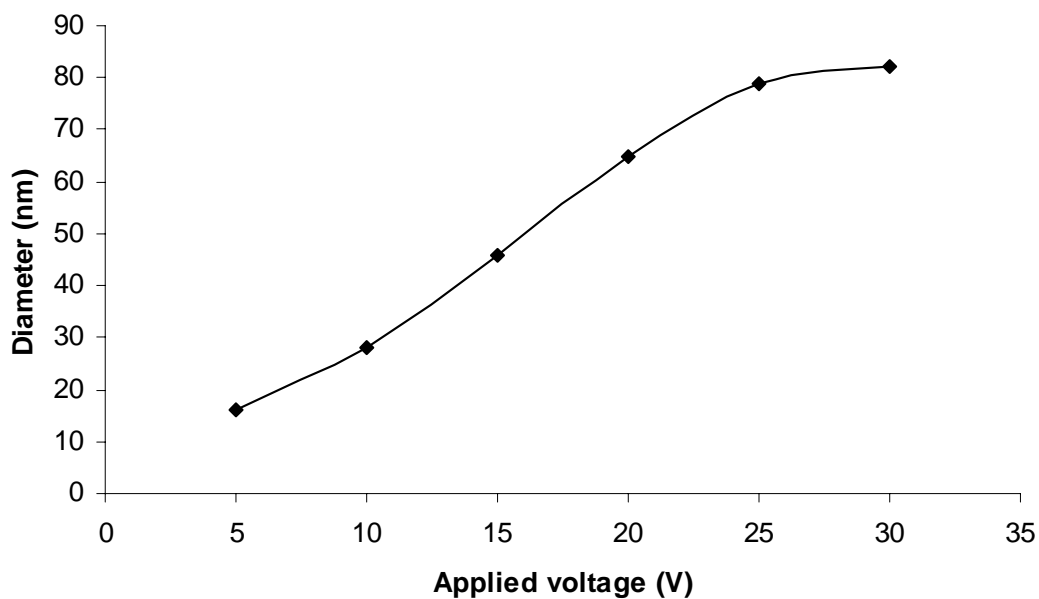


Figure 4: Surface of layers of self-aligned TiO<sub>2</sub> nanotubes with different diameters.

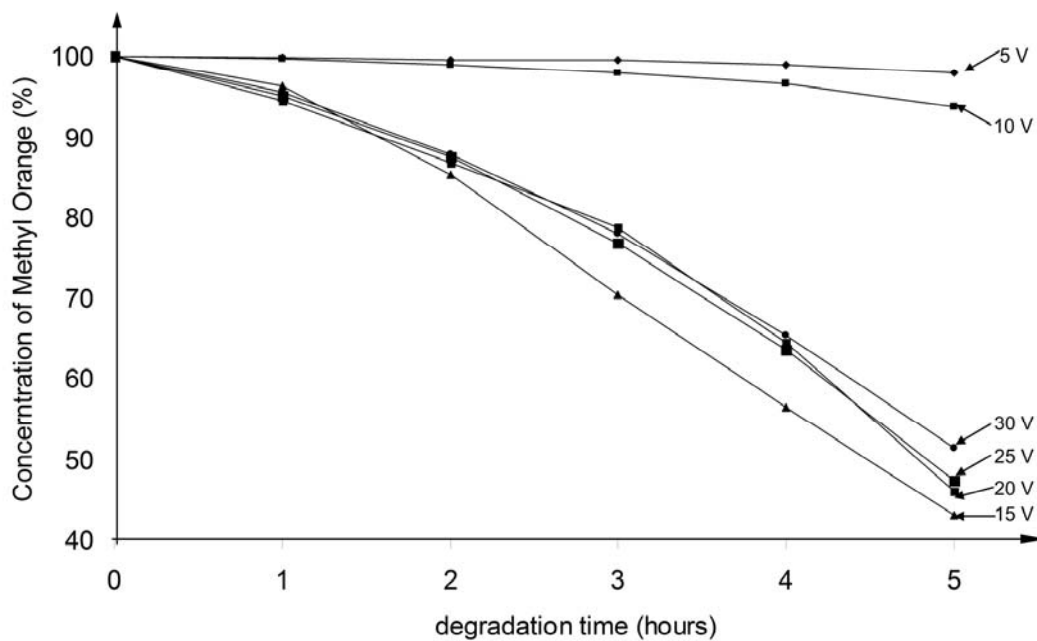


Figure 5: Plots of methyle orange concentration versus degradation time for TiO<sub>2</sub> nanotube produced at different voltage

## CONCLUSION

In order to produce self-array TiO<sub>2</sub> nanotubes layer for photocatalytic, anodizations were performed at various voltage from 5 V to 30 V. The current densities increase with increase of applied potential were noticed from 5 V to 30 V. Amorphous structures as-anodized self-organized TiO<sub>2</sub> nanotubes can be transformed to anatase upon annealing at 400 °C. The inner diameters of the nanotubes increased when the anodization voltages were increased and its start to remain almost constant after 25 V. TiO<sub>2</sub> nanotubes produces at 15 V show the greatest photocatalytic activity over the rest of another sample due to high surface area.

## ACKNOWLEDGEMENT

The author would like to thank Universiti Sains Malaysia because this work was sponsored through Short Term Grant 2007: 6035227 and FRGS: 6070020 and L' Oreal Fellowship

## REFERENCES

- [1]. N. Wang, X. Li, Y. Wang, X. Quan, G. Chen, (2008) *Chemical Engineering Journal* Article in Press
- [2]. K.O. Awitor, S. Rafqah, G. Géranton, Y. Sibaud, P.R. Larson, R.S.P. Bokalawela, J.D. Jernigen, M.B. Johnson, (2008) *Journal of Photochemistry and Photobiology A: Chemistry* **199** 250-254
- [3]. J. Yu, X. Zhao, J. Du, W. Chen, (2000) *Journal Sol-Gel Science and Technology* **17** 163-171
- [4]. K. Kato, A. Tsuzuki, Y. Torii, H. Taoda, (1995) *Journal of Materials Science* **30** 837-841
- [5]. Y.S. Sohn, Y.R. Smith, M. Misra, V.R. Subramanian, (2008) *Applied Catalysis B: Environmental* **84** 372-378
- [6]. J. Yu, X. Zhao, Q. Zhao, (2000) *Thin Solid Films* **379** 7-14
- [7]. Q. Chai, L. Yang, Y. Yu, (2006) *Thin Solid Films* **515** 1802-1806
- [8]. U. Černigoj, U.L. Štanger, P. Trebše, U.O. Krašovec, S. Gross, (2006) *Thin Solid Films* **495** 327-332
- [9]. B. Guo, Z. Liu, L. Hong, H. Jiang, J.Y. Lee (2005) *Thin Solid Films* **479** 310-315
- [10]. B. Guo, Z. Liu, L. Hong, H. Jiang (2005) *Surface & Coating Technology* **198** 24-29
- [11]. J.M. Macak and P. Schmuki, (2006) *Electrochimica Acta* **52** 1258-1264
- [12]. H.C. Liang, X.Z. Li, *Journal of Hazardous Materials* Article in Press
- [13]. C.K. Jung, I.S. Bae, Y.H. Song, T.K. Kim, J. Vlcek, J. Musil, J.H. Boo, (2005) *Surface & Coating Technology* **200** 534-538
- [14]. S. Sreekantan, R. Hazan, Z. Lockman, *Proceeding of 2nd International Conference & Exhibition on Composites Materials & Nano-structures*, (2008)

65

- [15]. D.J. Yang, H.G. Kim, S.J. Cho, W.Y. Choi, (2007) *Materials Letters* **62** 775-779
- [16]. V. Vega, M.A. Cerdeira, V.M. Prida, D. Alberts, N. Bordel, R. Pereiro, F. Mera, S. Carcía, M.H. Vélez, M. Vázquez, (2008) *Journal of Non-Crystalline Solids* **354** 5233-5235
- [17]. F.M. Bayoumi, B.G. Ateya, (2006) *Electrochemistry Communications* **8** 38-44
- [18]. J.M. Macak, L.V. Taveira, H. Tsuchiya, K. Sirotna, J. Macak, P. Schmuki, (2006) *Journal Electroceramic* **16** 29-34
- [19]. S.H. Kang, J.Y. Kim, H.S. Kim, Y.E. Sung, (2008) *Journal of Industrial and Engineering Chemistry* **14** 52-59